

INVESTIGATION OF LOCAL SPECTRAL DIFFERENCES BETWEEN CRITICAL AND DRIVEN SUB-CRITICAL CONFIGURATIONS IN MUSE-4

M. Plaschy, O.P. Joneja and R. Chawla

LRS, Paul Scherrer Institute, Villigen (PSI), and Swiss Federal Institute of Technology,
Lausanne (EPFL), Switzerland

G. Rimpault and C. Destouches

Nuclear Energy Division, CEA-Cadarache, St-Paul-lez-Durance, France

Abstract

Studies of spectral characteristics of different critical and driven sub-critical MUSE-4 configurations are presented in this paper. The current investigations have permitted to quantify important aspects, such as the influence of the intrinsic source, the asymmetry of the core along the north/south axis, the impact of the two different types of external sources to be employed, and the moderation/multiplication effects of the central diffusing lead region. One of the principal goals has been to define a suitable measurement programme using different threshold reaction rates and fission rate traverses (^{235}U and ^{238}U). These measurements will constitute an important experimental database for validating the calculational methods and data employed for analysing the neutron coupling in these ADS-representative configurations.

Introduction

In the context of waste management incorporating a transmutation option, accelerator-driven systems (ADS) represent an important alternative to conventional reactors due to their higher safety level when minor actinides such as neptunium and americium are loaded into the core. It has accordingly become necessary to extend the validation domain of calculational methods for critical fast reactors to the analysis of source-driven sub-critical configurations. The impact on the local neutron spectrum of new types of heterogeneities (e.g. a central lead region and a voided channel), and of the external source itself, must be adequately assessed for the accurate prediction of operational characteristics such as power peaking and irradiation damage effects.

In order to investigate such aspects, a large experimental programme, MUSE, has been established at the MASURCA facility at CEA-Cadarache (France). Certain phases of this programme have been already completed, [1-3] but the coupling of the $\text{PuO}_2/\text{UO}_2+\text{Na}$ core with an external neutron source of high intensity is currently being launched with the MUSE-4 phase. This has been achieved by employing a specially constructed neutron pulsed generator, called GENEPI, which produces neutrons via either a $\text{D}(\text{d},\text{n})\text{He}^3$ or a $\text{T}(\text{d},\text{n})\text{He}^4$ reaction. This paper presents, through MCNP4C Monte Carlo analysis [4] of simplified homogenised models, a comparison of spectral characteristics between the critical (reference), and three different sub-critical, MUSE-4 configurations. This spectral sensitivity study has provided the basis for the planning, and currently ongoing implementation, of a detailed programme of threshold-foil activation measurements in different selected locations.

The MUSE-4 configurations: description and modelling

This section presents the different critical and sub-critical MUSE-4 configurations employed for the current studies. The corresponding models for Monte Carlo simulation are also discussed.

Description

The different critical and sub-critical MUSE-4 configurations essentially consist of five different regions, each assembled from an arrangement of tubes of $10.6 \times 10.6 \times 230.44 \text{ cm}^3$, containing material representative of the region. It is convenient to describe the individual MUSE-4 regions starting from the inside of the assembly.

The presence of the accelerator tube at the centre creates a specific region, which crosses the reactor completely along the mid-plane. In front of the accelerator tube, which has a lead/aluminium clad, there is a lead diffusing region, which serves mainly to obtain a certain symmetry of the power distribution. These two regions, with their associated heterogeneity effects, represent ADS-specific particularities. The fuel zone consists of $\text{PuO}_2/\text{UO}_2+\text{Na}$ assemblies and is similar to a standard fast reactor core. Slightly different ^{239}Pu enrichments are employed for the fuel above and below the accelerator tube. A reflector region, constituted by sodium and stainless steel rods, surrounds the MOX zone. To obtain different criticality levels, some peripheral fuel assemblies are replaced by reflector assemblies. Finally the external zone of the reactor consists of stainless steel shielding. Horizontal cross-sectional views of the MUSE-4 critical and sub-critical configurations studied are given in Figure 1 and 2.

It is important to mention that the three different source-driven sub-critical levels SC1 ($k_{eff} = \sim 0.995$), SC2 ($k_{eff} = \sim 0.97$) and SC3 ($k_{eff} = \sim 0.95$), analysed in this study, correspond to the actual loadings planned for the MUSE-4 experimental programme. Moreover, in each sub-critical configuration, the deuteron pulsed accelerator (GENEPI) will be used in each of the two different possible modes, viz. to produce neutrons of either 2.58 MeV via the $D(d,n)He^3$ reaction or of 14.16 MeV via the $T(d,n)He^4$ reaction.

MCNP4C modelling

MCNP4C is a widely used stochastic code. One of its main advantages is the ability to accurately describe the experimental configuration, e.g. modelling complicated shapes having several heterogeneous building blocks such as the accelerator zone. However, the computing time can be very significant with the statistical approach, particularly in obtaining adequate uncertainties for threshold reaction rates. The current MCNP4C analysis has been carried out using the JEF-2.2 library with updated data for ^{239}Pu .

The geometry and material descriptions for creating the numerical MCNP models have been taken from a document [5] presenting the specifications for a new international benchmark exercise based on MUSE-4. Preliminary results of this benchmark have indicated that the calculational scheme used here is indeed quite satisfactory.

The MCNP4C calculations have been carried out in the KCODE and/or SOURCE modes, depending on the type of studied configuration and results desired. For the SOURCE calculations, different models have been used to describe the external source. First of all, a simple model has been used, with the source considered to be isotropic in space and having an energy of 2.58 MeV or 14.16 MeV. Later, improved and more representative modelling has been done considering the anisotropy of the sources, as assessed from standard kinematic calculations. For the spatial dependency, the intensity variation between the most and the least favourable directions is about 20% for the $D(d,n)He^3$ reaction, and less than 7% for the $T(d,n)He^4$. For the anisotropy in energy, the spread is from 2.1 MeV to 3 MeV for $D(d,n)He^3$, and from 13.1 MeV to 15.1 MeV for $T(d,n)He^4$. Finally, it is also important to take into account the intrinsic source of the reactor, which is due to the spontaneous fissions and (α,n) reactions resulting from the disintegration of specific nuclides in the MOX fuel. This source has been represented with the help of a recent study carried out at Cadarache. [6] The actual source intensities are to be measured during the MUSE-4 programme, the expected representative values used in this study being: $5.0E+08$ n/s for $D(d,n)He^3$, $1.0E+10$ n/s for $T(d,n)He^4$ and $2.0E+08$ n/s for the intrinsic source.

As mentioned earlier, the present comparisons of MCNP4C results for the different critical and sub-critical MUSE-4 configurations are meant to quantify various effects, such as the impact of the external source, on the predictions of spectral variations in the system. Furthermore, clear identification is being sought of the locations at which these spectral variations are particularly important, so that the planning of specific measurements, e.g. with activation foils, can be most effective. In general, such investigations are difficult to carry out accurately with deterministic codes in these sub-critical heterogeneous driven systems.

Calculations and discussion

Different calculations have been performed in the critical and sub-critical MUSE-4 configurations. Firstly, the results are given for k_{eff} and for power values in the sub-critical

configurations. Then, certain spectral characteristics of the core are presented through several reaction rate traverses. Finally, results are given for different threshold reaction rates at specific locations to illustrate the manner in which the planning of the foil activation programme has been conducted.

Determination of the k_{eff} and the power

The calculated values of k_{eff} are given in Table 1. The results are expected to be quite reliable in general, considering that the critical configuration has already been confirmed experimentally (corrected experimental $k_{eff} = \sim 0.999$).

The results for the power of the sub-critical configurations in Table 2 permit an estimation to be made of the contribution of the intrinsic source to the total power in each case. Thus, about 30% of the fission power is due to the intrinsic source when the system is driven by the $D(d,n)He^3$ source, but the figure is less than 1% in the case of the $T(d,n)He^4$ source. Of course, this is principally due to the different intensities of the two external sources. Nevertheless, the emitted spectrum and the different source geometry (external/intrinsic) have significant effects. Effectively, the ratio of the intensities for the $T(d,n)He^4$ source and the intrinsic source is 50 ($1.0E+10/2.0E+8$), while the ratio of the resulting power is greater than 100 (see Table 2). The impact of the intrinsic source on different reaction rates is given in the next section.

Spectral characterisation of the core and contribution of the different source

The east/west and north/south channels, indicated in Figure 1, represent the accessible horizontal experimental channels in which measurements could be performed. For axial traverses, it is possible to create an experimental channel by removing some rodlets from a tube at a given position of interest. In this section, certain results for configurations CRIT (critical loading), SC2 and SC3 are presented to clearly identify the impact of the sub-critical level in the two horizontal channels and at specific locations.

^{238}U and ^{235}U fission traverses along the west/east axis are presented in Figure 3. Normalisation has been done by adjusting the sum of the point values calculated for each configuration to 1.0 (statistical uncertainty is less than 1.5% for each point between -40 cm and 40 cm). The presence of the external source and the level of sub-criticality is reflected most clearly in the different shapes of the ^{238}U fission rate traverses in the three configurations. Effectively, the decrease of this threshold fission reaction in lead, which appears in the case of the CRIT configuration (moderation effect of lead), is replaced by significant peaking effects in the driven sub-critical configurations. Moreover, this effect is higher for a more sub-critical system, because of the reduced impact of the fuel region. The ^{235}U fission rate west/east traverse principally indicates the reflector effect and, as such, is characteristic of the different number of fuel assemblies in each case. Finally, there is no significant difference in the ^{235}U and ^{238}U fission rates due to the specific use of the $D(d,n)He^3$ or $T(d,n)He^4$ sources. This fact underlines the desirability of carrying out a wider range of measurements, e.g. using specific activation foils, as described below.

The $^{238}U/^{235}U$ fission ratio is presented as spectral index in Figure 4 along the symmetrical west/east and the asymmetrical north/south axes. At the centre, a change by a factor of about two in this specific ratio is reached between critical and sub-critical systems. This difference is clearly much larger than any experimental uncertainties, such that important validation results can be expected from measurements at this location. The study of the north/south axis permits to see the asymmetry of the core due to the lead and accelerator tube regions. However, the asymmetry is highlighted when the

external source is active. This particular behaviour is characteristic of a hybrid system and seems well predicted by Monte Carlo codes, while it is often a difficulty with deterministic methods (treatment of voided regions). The $^{238}\text{U}/^{235}\text{U}$ spectral index has been calculated with the two (isotropic and anisotropic) models of the external source, but no impact has been identified, as indicated in Figure 4. In fact, significant differences are present only when higher threshold reactions are considered.

The presence of an intrinsic source in a MASURCA core has already created some interpretation problems in the past, viz. when the system was used in a sub-critical mode with an external source of weak intensity. It has been reported [7] that the uncertainty of about 30% attached to the intrinsic source determination was the basic cause of the difficulty. For our case, an assessment of the importance of the intrinsic source on several reaction rates is presented in Table 3 for the SC2 configuration driven by the $\text{D}(\text{d},\text{n})\text{He}^3$ source. As the intensity of the $\text{T}(\text{d},\text{n})\text{He}^4$ source is much higher, the presence of the intrinsic source brings no significant contribution to the global uncertainty of any reaction rate results (<0.5%). However, Table 3 shows that the contribution of the intrinsic source, when the $\text{D}(\text{d},\text{n})\text{He}^3$ source is used, is always around 25 to 30% for thermal and threshold reactions at locations 1, 5 and 6 (see Figure 1). However, the impact reduces to less than 5% for threshold reactions at location 2. In the symmetrical locations 3 and 4, the influence of the intrinsic source is also slightly reduced for the threshold reactions. Consequently, the uncertainties introduced for the case of $\text{D}(\text{d},\text{n})\text{He}^3$ are around 1.5% for threshold reactions near the external source but they are increased here up to 10% for thermal reactions. The increase in uncertainty is general for locations which are away from the external source. Taking into account these considerations, it is evident that spectral studies of the accelerator/core coupling, can be expected to be much more reliable for the $\text{T}(\text{d},\text{n})\text{He}^4$ -driven MUSE-4 configurations.

Definition of an appropriate experimental programme for the MUSE-4 configurations

It is indeed the interpretation of various calculated ratios and spectral indices of the above type which has led to the final definition of the programme of foil-activation measurements in MUSE-4. The choice of the locations indicated in Figure 1 has been made on the basis of the exhaustive set of MCNP4C simulations and is meant to be representative, in a generic sense, of different aspects of interest, as described below:

Location 1:	Relatively unperturbed core position.
Location 2:	External source influence, moderation/multiplication effects of lead.
Locations 3 & 4:	Core asymmetry and anisotropy of the external source.
Location 5:	Lead moderation/multiplication effects.
Location 6:	Streaming effects in the voided channel.
Location A:	Reflector effects.
Locations B, C & D:	Variations along the west/east axis.

The choice of foils has been guided mainly by the need to cover as wide a range of threshold energy values as possible. The complete range of special activation foils and reactions to be employed in the MUSE-4 investigations is presented in Table 4 (some others complementary foils will be added in the locations A, B, C & D: ^{232}Th , ^{235}U , ^{237}Np ,...).

For illustration, Table 5 gives an indication of the activity ratios, expressed relative to the reference location 1 as predicted for various positions and for several different types of thermal and threshold reactions in the three MUSE-4 configurations. The impact of the external source on these ratios is clearly highlighted. In particular, the ratios are much more larger near the external source

(location 2) and when the $T(d,n)He^4$ source is implemented (red values of Table 5). Furthermore, the selected threshold activation foils permit to separate the spectral effects due to the $D(d,n)He^3$ and $T(d,n)He^4$ reactions, which was not possible with standard ^{235}U or ^{238}U fission reactions (see Figures 3 and 4). This is illustrated principally by the $^{56}Fe(n,p)$, $Mg^{24}(n,p)$ and $^{51}V(n,\alpha)$ threshold reaction rates of Table 5. Additionally, this Table shows that the more sub-critical the system, the more important is the external source contribution. Effectively, for a given source type, the threshold reaction ratios near the central region (2/1, 3/1 and 4/1) are always higher in the SC3 configuration in comparison with the SC2. Moreover, the north/south asymmetry of the core is clearly seen in comparing the ratios 3/1 and 4/1. For example, the high-threshold reaction rate ratios 4/1 are significantly increased when the $T(d,n)He^4$ reaction is used, indicating a certain streaming effect along the voided accelerator channel (pink values of Table 5). However, this effect disappears when a location further away is considered (ratio 6/1). In the south part of the core, the ratio 5/1 marks the distance beyond which almost no influence of the external source can be seen. Finally, others physical aspects, like the moderation effect of lead, can be estimated by foil activation studies, as indicated by the 2/1 and 3/1 ratios, in the reference critical configuration. There, the value for the non-threshold reaction rate $^{197}Au(n,\gamma)$ is greater than 1.0 and those for the higher-threshold reactions is lower than 1.0.

In brief, it has been demonstrated that the use of specific threshold reactions permits to highlight the different influence of each external source. This justifies the interest of such measurements to analyse the accelerator/core coupling in MUSE-4 from the viewpoint of the spectral variations to be expected in a hybrid system. The currently discussed simulations for defining measurement locations and foil materials of interest have, of course, been complemented by feasibility studies (for example calculations of effective cross-sections and flux levels) to propose an appropriate foil activation measurement programme in MUSE-4. This has led to preferentially choose the following configurations for the experiments: REF, SC1 (with both $D(d,n)He^3$ and $T(d,n)He^4$ sources), SC2 (with the $T(d,n)He^4$ source only). Some measurements have already been performed in the critical loading without any external source, [8] and planning for the measurement programmes in the sub-critical MUSE-4 configurations is complete. Finally, it should be mentioned that one other goal of the foil activation techniques is to obtain, by applying appropriate unfolding techniques, [9] the higher energy neutron spectrum at different locations, and to compare these results between the different MUSE-4 configurations.

Conclusions

This paper has analysed some of the local spectral differences between critical and driven sub-critical MUSE-4 configurations. The impact of specific regions of the system (accelerator tube, lead, etc) on the spectrum has been studied. For example, the lead moderation/multiplication effects and the impact of the external source have been quantified through analysis of different reaction rates. Also, the contribution of the intrinsic source, due to the MOX fuel, has been evaluated. It is demonstrated that this neutronic component brings significant uncertainty when the $D(d,n)He^3$ reaction is used. Finally, the characterisation of the core, through calculations of various spectral indices, has led to define the final programme of foil activation measurements in the MUSE-4 configurations. It has also been shown in this study that the planned measurements are more appropriate for analysing the influence of the external source and the impact of the sub-criticality level than are standard fission rate traverses.

REFERENCES

- [1] M. Salvatores *et al.* (1996), *MUSE-1: A First Experiment at MASURCA to Validate the Physics of Sub-critical Multiplying Systems Relevant to ADS*, Proc. 2nd Int. Conf. Accelerator-driven Transmutation Technologies and Application, Kalmar, Sweden.
- [2] R. Soule *et al.* (1997), *Validation of Neutronics Method Applied to the Analysis of Fast Sub-critical Systems: The MUSE-2 Experiments*, Proc. GLOBAL'97, Yokohama, Japan.
- [3] J.F. Lebrat *et al.* (1999), *Experiment Investigation of Multiplying Sub-critical Media in Presence of an External Source Operating in Pulsed or Continuous Mode: The MUSE-3 Experiment*, Proc. 3rd Int. Conf. Accelerator-driven Transmutation Technologies and Application, Praha, Czechia.
- [4] J.F. Briesmeister (1993), *MCNP – A General Monte Carlo N-Particle Transport Code*, Los Alamos National Laboratory Report LA-12625.
- [5] D. Villamarin *et al.* (2001), *Benchmark on Computer Simulation of MASURCA Critical and Sub-critical Experiments (MUSE-4 BENCHMARK)*, NEA/OECD-WPPT(2001)5, Paris, France.
- [6] R. Babut (2001), *Modeling of (α,n) Reactions on Light Nuclei and Preliminary Results*, Int. Conf. on Nuclear Data for Science and Technology, Tsukuba, Japan.
- [7] G. Aliberti (2001), *Caractérisation neutronique des systèmes hybrides en régimes stationnaire et transitoire*, Thèse de l'Université Louis Pasteur, Strasbourg.
- [8] M. Plaschy *et al.* (2002), *Foil Activation Studies of Spectral Variations in the MUSE-4 Critical Configuration*, Proc. PHYSOR'02, Seoul, Korea.
- [9] U. Hong *et al.* (1999), *Measurements of Neutron Spectrum in HANARO*, Proc. Reactor Dosimetry: Radiation Metrology and Assessment, Osaka, Japan.

Figure 1. **Horizontal cross-sectional view of the MUSE-4 critical configuration, indicating the foil locations and the experimental channels** (each of the square cells is 10.6 cm×10.6 cm)

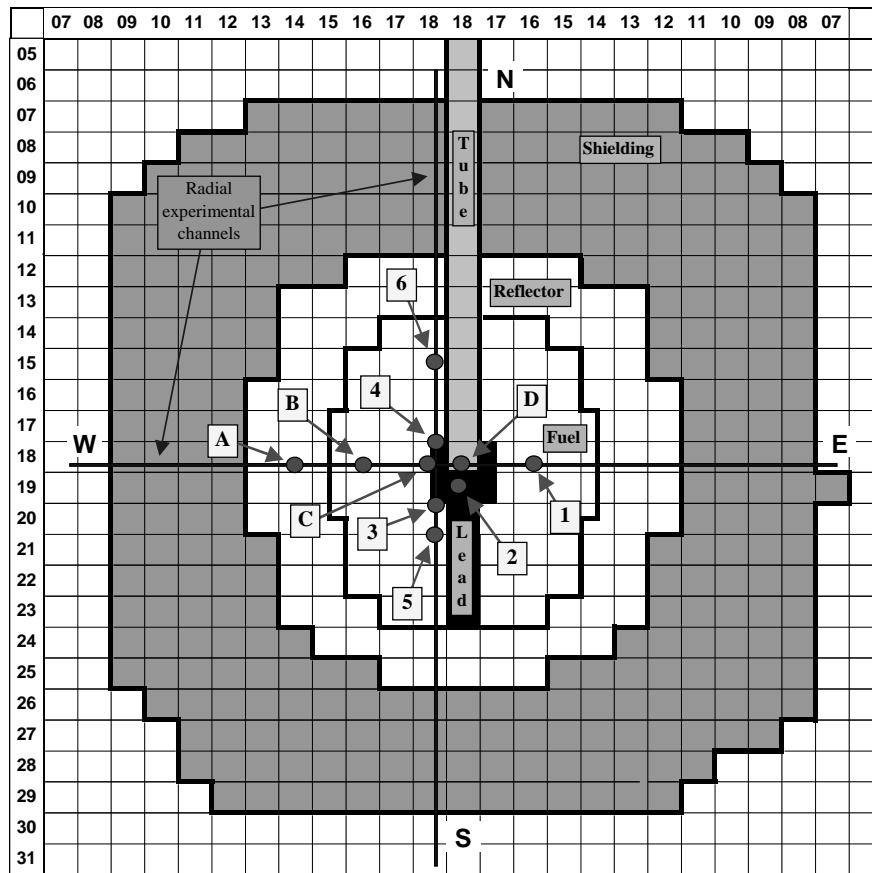


Figure 2. **Horizontal cross-sectional view of the sub-critical MUSE-4 cores, SC1, SC2 and SC3**

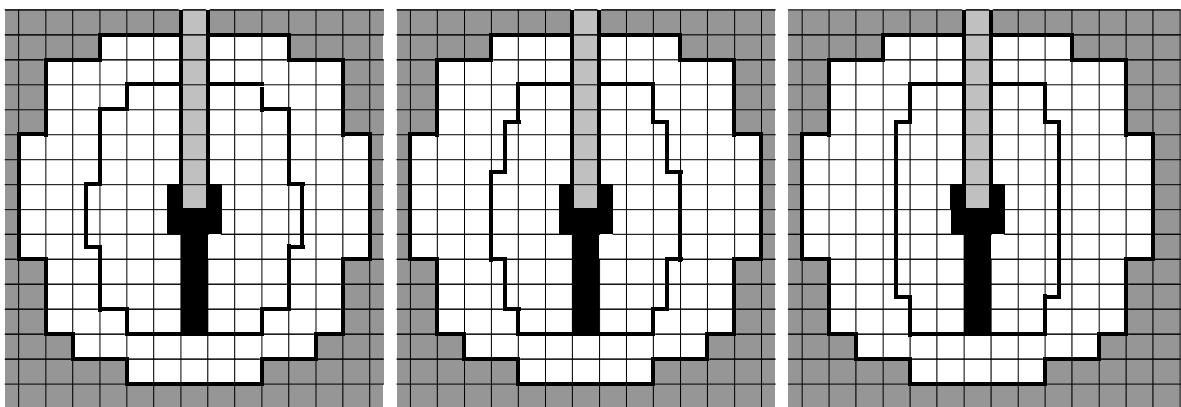


Figure 3. ^{238}U and ^{235}U fission rate traverses along the west/east axis

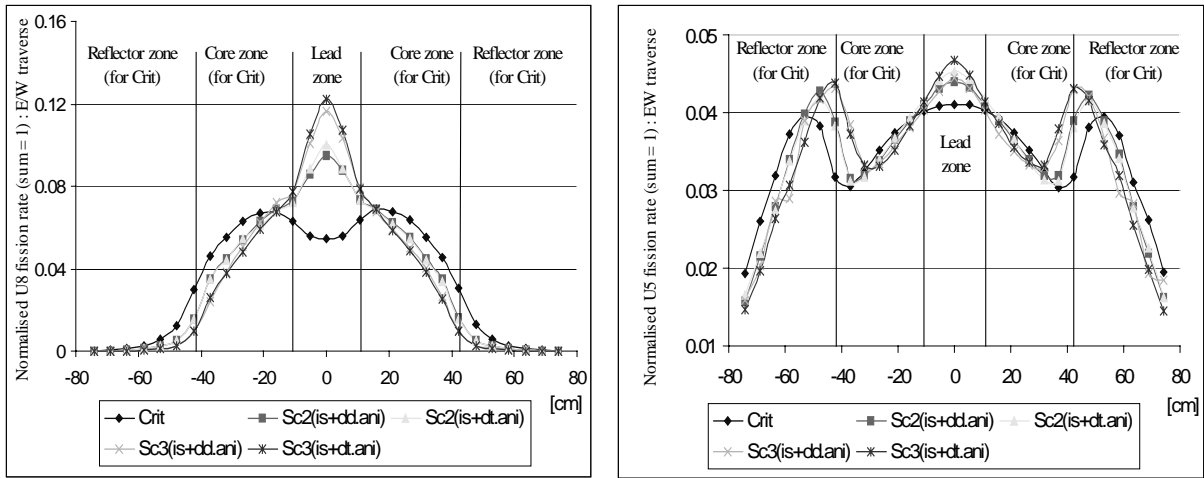


Figure 4. Calculated $^{238}\text{U}/^{235}\text{U}$ fission ratio variations along the two horizontal channels

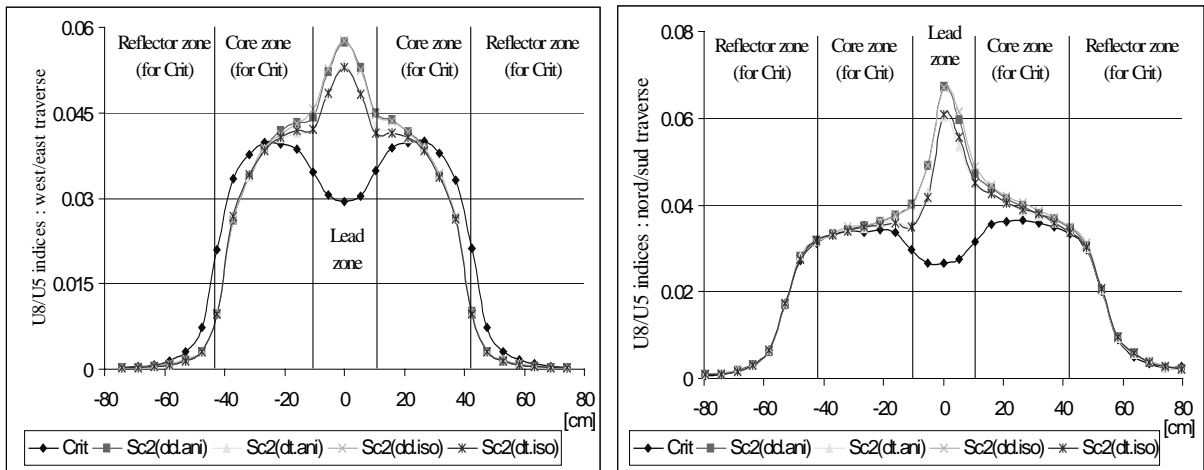


Table 1. Calculated (MCNP-4C) k_{eff} values for the investigated MUSE-4 configurations

MUSE-4 configuration	Used code and library	k_{eff}
REF	MCNP-4C + Jef-2.2	$1.00024 \pm 12\text{pcm}$
SC1	MCNP-4C + Jef-2.2	$0.99515 \pm 41\text{pcm}$
SC2	MCNP-4C + Jef-2.2	$0.96937 \pm 30\text{pcm}$
SC3	MCNP-4C + Jef-2.2	$0.94957 \pm 27\text{pcm}$

Table 2. Calculated (MCNP-4C) power values for the investigated MUSE-4 configurations

MUSE-4 configuration	Implemented source	Power
SC1	Intrinsic source (is)	~0.30 W
SC1	Anisotropic dd source (dd.ani)	~1.05 W
SC1	Anisotropic dt source (dt.ani)	~34.90 W
SC2	Intrinsic source (is)	~0.06 W
SC2	Anisotropic dd source (dd.ani)	~0.21 W
SC2	Anisotropic dt source (dt.ani)	~7.10 W
SC3	Intrinsic source (is)	~0.04 W
SC3	Anisotropic dd source (dd.ani)	~0.14 W
SC3	Anisotropic dt source (dt.ani)	~4.50 W

Table 3. Assessment of the intrinsic source (is) contribution, as compared to that due to the D(d,n)He3 source (dd), for different reactions and locations in the SC2 configuration (ratio is/dd)

Location Reaction	1 (is/dd)	2 (is/dd)	3 (is/dd)	4 (is/dd)	5 (is/dd)	6 (is/dd)	1-σ : for all%
$^{197}\text{Au}(n,\gamma)^{198}\text{Au}$	0.27	0.26	0.27	0.29	0.29	0.29	<3.7
$^{115}\text{In}(n,n')^{115\text{m}}\text{In}$	0.27	0.11	0.21	0.20	0.28	0.28	<2.4
$^{58}\text{Ni}(n,p)^{58}\text{Co}$	0.27	0.04	0.21	0.22	0.27	0.28	<2.3
$^{235}\text{U}(n,\text{fis})$	0.26	0.21	0.27	0.26	0.29	0.28	<1.6
$^{238}\text{U}(n,\text{fis})$	0.24	0.05	0.20	0.17	0.27	0.27	<2.1

Table 4. List of special foils and reactions to be employed for spectral studies in MUSE-4 (Locations 1 to 6)

Selected foils to cover a large energy range			
Reactions	Threshold (MeV)	Reactions	Threshold (MeV)
$^{197}\text{Au}(n,\gamma)^{198}\text{Au}$	/	$^{54}\text{Fe}(n,p)^{54}\text{Mn}$	3.1
$^{59}\text{Co}(n,\gamma)^{60}\text{Co}$	/	$^{56}\text{Fe}(n,p)^{56}\text{Mn}$	6.0
$^{64}\text{Zn}(n,\gamma)^{65}\text{Zn}$	/	$^{24}\text{Mg}(n,p)^{24}\text{Na}$	6.8
$^{115}\text{In}(n,\gamma)^{116\text{m}}\text{In}$	/	$^{27}\text{Al}(n,a)^{24}\text{Na}$	7.2
$^{115}\text{In}(n,n')^{115\text{m}}\text{In}$	1.2	$^{59}\text{Co}(n,2n)^{58}\text{Co}$	10.6
$^{59}\text{Co}(n,p)^{59}\text{Fe}$	2.0	$^{93}\text{Nb}(n,2n)^{92\text{m}}\text{Nb}$	11.0
$\text{Zn}^{64}(n,p)^{64}\text{Cu}$	2.8	$^{51}\text{V}(n,\alpha)^{48}\text{Sc}$	11.5
$\text{Ni}^{58}(n,p)^{58}\text{Co}$	2.8	$^{58}\text{Ni}(n,2n)^{57}\text{Ni}$	13.5

Table 5. Activity ratios for different threshold reactions at various locations of the MUSE-4 configurations

Ratio	Config.	$^{197}\text{Au}(n,\gamma)$	$^{115}\text{In}(n,n')$	$^{58}\text{Ni}(n,p)$	$^{56}\text{Fe}(n,p)$	$^{24}\text{Mg}(n,p)$	$^{51}\text{V}(n,\alpha)$
2/1	CRIT (/)	1.22 ±0.02	0.66 ±0.01	0.44 ±0.01	0.21 ±0.01	0.18 ±0.02	0.25 ±0.04
	SC2 (dd)	1.25 ±0.04	3.24 ±0.03	3.27 ±0.03	0.18 ±0.01	0.14 ±0.02	0.12 ±0.02
	SC2 (dt)	1.23 ±0.04	2.41 ±0.02	2.74 ±0.03	26.61 ±1.06	33.22 ±1.99	74.00 ±4.44
	SC3 (dd)	1.15 ±0.04	4.52 ±0.04	4.78 ±0.05	0.22 ±0.02	0.17 ±0.02	0.18 ±0.02
	SC3 (dt)	1.10 ±0.04	3.39 ±0.04	3.96 ±0.04	32.91 ±1.31	39.24 ±2.23	77.64 ±6.21
3/1	CRIT (/)	1.16 ±0.02	0.83 ±0.01	0.70 ±0.01	0.56 ±0.03	0.53 ±0.04	0.56 ±0.05
	SC2 (dd)	1.15 ±0.04	1.11 ±0.01	0.93 ±0.02	0.55 ±0.03	0.54 ±0.05	0.65 ±0.06
	SC2 (dt)	1.15 ±0.04	1.02 ±0.01	0.87 ±0.02	1.40 ±0.08	1.57 ±0.10	2.76 ±0.19
	SC3 (dd)	1.05 ±0.05	1.25 ±0.01	1.08 ±0.02	0.58 ±0.03	0.55 ±0.05	0.68 ±0.06
	SC3 (dt)	1.01 ±0.04	1.14 ±0.01	0.97 ±0.02	1.63 ±0.09	2.21 ±0.13	2.98 ±0.24
4/1	CRIT (/)	1.14 ±0.02	0.85 ±0.01	0.74 ±0.01	0.60 ±0.03	0.58 ±0.04	0.65 ±0.05
	SC2 (dd)	1.08 ±0.06	1.19 ±0.01	0.95 ±0.02	0.63 ±0.03	0.60 ±0.05	0.72 ±0.05
	SC2 (dt)	1.11 ±0.04	1.20 ±0.01	1.26 ±0.02	5.09 ±0.25	6.30 ±0.38	8.05 ±0.48
	SC3 (dd)	1.07 ±0.06	1.51 ±0.02	1.12 ±0.02	0.72 ±0.04	0.73 ±0.06	0.80 ±0.05
	SC3 (dt)	0.98 ±0.04	1.40 ±0.01	1.53 ±0.02	6.13 ±0.31	7.31 ±0.32	8.38 ±0.69
5/1	CRIT (/)	1.07 ±0.02	0.88 ±0.01	0.82 ±0.01	0.77 ±0.03	0.77 ±0.05	0.87 ±0.07
	SC2 (dd)	1.03 ±0.06	0.90 ±0.01	0.85 ±0.02	0.75 ±0.04	0.73 ±0.05	0.83 ±0.10
	SC2 (dt)	1.03 ±0.04	0.92 ±0.01	0.85 ±0.02	0.63 ±0.04	0.58 ±0.04	0.58 ±0.07
	SC3 (dd)	0.93 ±0.05	0.92 ±0.01	0.87 ±0.02	0.81 ±0.05	0.83 ±0.05	0.85 ±0.10
	SC3 (dt)	0.86 ±0.05	0.93 ±0.01	0.84 ±0.02	0.58 ±0.04	0.52 ±0.04	0.54 ±0.07
6/1	CRIT (/)	0.87 ±0.02	0.71 ±0.01	0.68 ±0.01	0.67 ±0.03	0.69 ±0.03	0.80 ±0.07
	SC2 (dd)	0.80 ±0.05	0.70 ±0.01	0.68 ±0.02	0.67 ±0.03	0.68 ±0.04	0.73 ±0.05
	SC2 (dt)	0.88 ±0.03	0.71 ±0.01	0.69 ±0.02	0.71 ±0.03	0.71 ±0.04	0.62 ±0.05
	SC3 (dd)	0.79 ±0.05	0.74 ±0.01	0.71 ±0.02	0.69 ±0.03	0.70 ±0.04	0.72 ±0.05
	SC3 (dt)	0.83 ±0.03	0.74 ±0.01	0.71 ±0.02	0.70 ±0.03	0.68 ±0.04	0.59 ±0.05

0.0 < X < 0.5: Blue
 0.5 < X < 1.0: Black
 1.0 < X < 2.0: Green
 2.0 < X < 5.0: Turquoise
 5.0 < X < 10.0: Pink
 10.0 < X : Red